Multi-Photon Spectroscopy on Xenon for Application on Ion Thruster Plasma Parameter Investigations: Experiment and Theory

IEPC-2007-169

Presented at the 30th International Electric Propulsion Conference, Florence, Italy
September 17-20, 2007

Christoph Eichhorn* and Michael Winter†
Institut für Raumfahrtsysteme IRS, Universität Stuttgart, Pfaffenwaldring 31, D-70569 Stuttgart, Germany

Monika Auweter-Kurtz‡
Universität Hamburg, Edmund-Siemers-Allee 1, D-20196 Hamburg, Germany

and

Stefan Löhle§
DLR Institut für Verbrennungstechnik, Pfaffenwaldring 38-40, D-70569 Stuttgart, Germany

Three excitation schemes for two-photon laser-induced fluorescence (TALIF) on neutral xenon involving $6p'$ and $7p$ states are presented. An overview on possible transitions is given. In addition to the well-known transition at $\lambda = 2 \times 225.5$ nm, two alternative candidates for neutral xenon ground state diagnostics are experimentally investigated in a xenon-filled cold gas cell. It was found that alternative excitation schemes showed remarkable signal intensities and can be used for future TALIF measurements in neutral xenon additionally. Some theoretical aspects of three-photon spectroscopy with respect to singly ionized xenon ground state diagnostics are discussed. Three-photon transition rates are expected to have transition rates about ten orders of magnitude lower than those of two-photon processes.

I. Introduction

Regarding the quantitative determination of time- and space resolved particle densities, laser-induced fluorescence (LIF) spectroscopy occupies a position of significant importance as a diagnostic method to study physical processes in complicated plasma states. At IRS, recent investigations have been concentrated on two-photon absorption laser-induced fluorescence (TALIF) detection of atomic oxygen in inductively heated oxygen plasma flows as well as in inductively heated air flows to study re-entry plasma conditions.[1–3] Besides, the detection of neutral xenon (Xe I) has been performed in a cold gas cell, representing a test environment for later application for xenon-operated ion thruster diagnostics.[4] In addition, cold-gas cell measurements of Xe I have been used to calibrate atomic oxygen densities.[2]

The necessity to involve multi-photon excitation processes in LIF diagnostics arises for a multitude of atomic species possessing a high energy gap between the ground state and the first excited state. As population densities of atomic levels are usually not known in complicated plasma states, particle densities

*PhD student, eichhorn@irs.uni-stuttgart.de
†Research scientist
‡Professor, President Universität Hamburg
§Research scientist

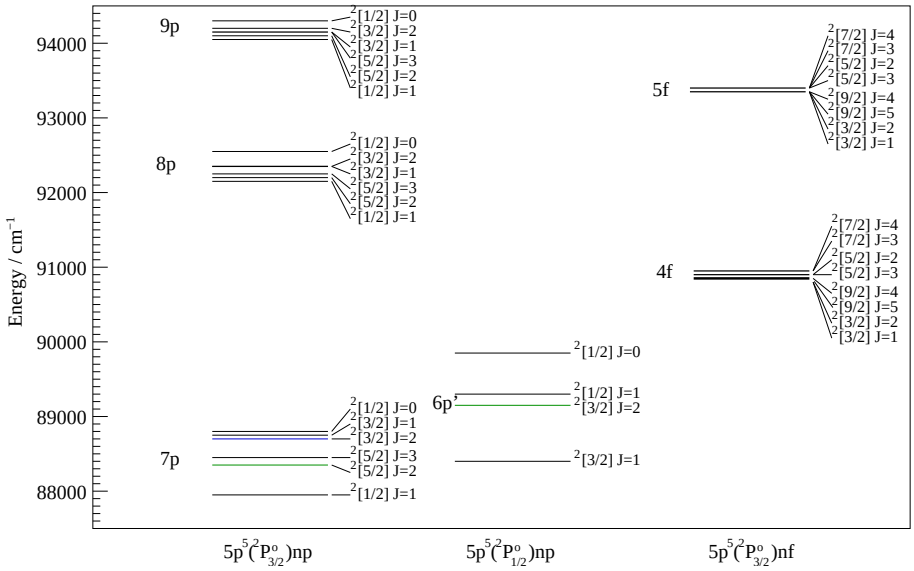

Figure 1. Energy levels of Xe I with even parity between 87500 cm^{-1} and 94500 cm^{-1}. Traditional and alternative levels are emphasized blue and green, respectively.

can not be found by exciting arbitrary transitions. However, excitation from the ground state allows the calculation of particle densities if the ground state can be assumed to be not significantly depopulated at moderate plasma temperatures. Considering diagnostics of xenon plasmas being existent in the plume of ion thrusters like Radio-Frequency Ion Thruster (RIT), expected particle densities are extremely low. Moreover, only neutral xenon species (Xe I) are able to be detected with TALIF, while, for the singly-ionized species (Xe II), a three-photon excitation LIF scheme is required due to the fact that the first non-forbidden excitation from the ground state corresponds to $\lambda \lesssim 90$ nm. As in the case of atomic oxygen measurements, the problem of naturally low excitation probabilities is combined with special requirements on the experimental environment. Experimental facilities aiming at plasma diagnostics of electric thrusters are hard to compare to those in physical laboratories, as, for example, significantly longer optical paths to the excitation volume are necessary, limiting excitation and detection efficiencies. The reference to experiments related to three-photon spectroscopy on xenon published in a remarkable variety in the physical literature[5–7], is therefore problematic.

With respect to low particle densities expected in ion thruster plasma plumes and small absorption cross sections for multi-photon processes, the choice of a possibly efficient (TA-)LIF scheme becomes an important issue. Fig. 1 shows levels that fulfill the parity selection rule for two-photon excitation from the ground state for Xe I (however, additional selection rules have to be considered, see following section). Detection can be performed by two-photon excitation of the $5p^5(^2P^\circ_{3/2})7p\ ^2[3/2]_2$-level at 88686.5 cm^{-1} (referring to 2×225.5 nm photons), which is well understood[8,9] and has been used by Crofton[10] in a study of Xe I particle densities in a T5 ion thruster plume. Within this paper, first results of alternative TALIF schemes including two additional $6p'$ and $7p$ J=2 states are discussed (highlighted green in Fig. 1). Some remarks on three-photon processes are given.

II. Theory

A. Fluorescence Formula for TALIF in the Kinetic Model

Modelling a two-photon laser-induced fluorescence process using a system of rate equations, what is appropriate as long as no saturation of the absorption process occurs, has been described well in literature[11]. In a model including the two-photon excitation from the ground state, fluorescence decay of the two-photon excited state and possible photoionization of the two-photon-excited state, the fluorescence signal S is given

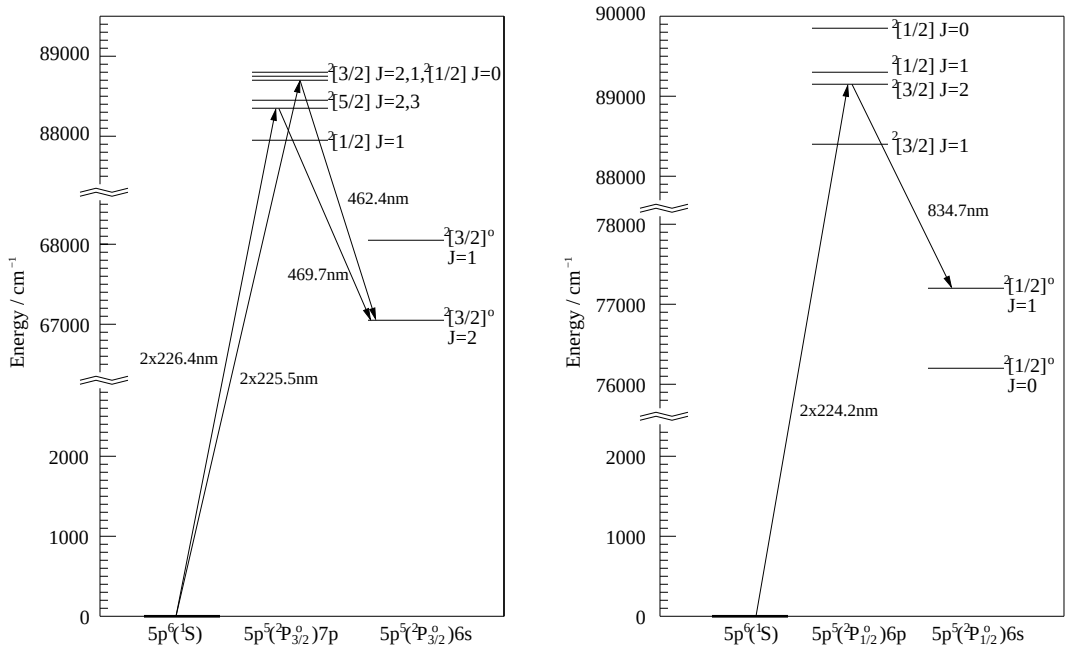

Figure 2. Three possible excitation schemes for TALIF on Xe I in the excitation range 224nm $< \lambda <$ 227 nm.

by

$$S = D\,\frac{E^2}{a^2}\,\frac{A_{21}}{A+Q}\,\frac{\hat{\sigma}^{(2)} n_0}{4\pi^2(\hbar\omega)^2}\int_{-\infty}^{\infty} F^2(t)dt \tag{1}$$

wherein E is the energy of the laser pulse, a the beam waist at the detection area, n_0 the particle density, ω and $F(t)$ the frequency and the temporal profile of the laser beam respectively, A_{21} the Einstein coefficient for the fluorescence transition, Q the quenching rate and $\hat{\sigma}^{(2)}$ the two-photon absorption cross section. If the temporal profile of the laser beam is well described by a Gaussian, the integral can be evaluated by $\int F^2(t)dt = (\sqrt{\pi}\tau_p)^{-1}$, denoting τ_p the FWHM duration of a laser pulse. The calibration constant D includes all factors with influence on the sensitivity to the detection system,

$$D = L\Omega\eta_t\eta_\Phi eKG_p\frac{G_a}{C}, \tag{2}$$

with η_t denoting the transmission function of all windows and filters, η_Φ the quantum efficiency of the photomultiplier, G_p the photomultiplier tube gain, K including preamplifier gain and sensitivities of further analyzing instruments, G_a/C the ratio of preamplifier to capacitance (in V/C), e the elementary charge (in C), L the effective length of the light collection system (in cm) and Ω the solid angle (in sr) of the collection lens. The units of S and D are V and V·cm·sr, respectively.

B. TALIF Excitation Schemes for Xenon

TALIF excitation schemes have to satisfy two-photon electric dipole selection rules. As the most general one, the parity rule requests a transition between two states of the same parity. The ground state of Xe I is of even parity. In Fig. (1), the complete energy levels of even parity are shown in the range between 87500 cm^{-1} and 94500 cm^{-1}. Angular momentum selection rules require a variation of the total orbital angular momentum $\Delta L = 0, \pm 2$ and the total electronic angular momentum $|\Delta J| \leq 2$. It must be noted that the polarizations of the two photons can become important, since some transitions are allowed only if they differ in polarization orientation. In the case of two photons with the same frequencies and polarizations (as existing in our experiment), additionally $\Delta J : 0 \leftrightarrow 1$ is forbidden. For a complete derivation and discussion of two-photon dipole selection rules, see Bonin and McIlrath[12].

From Eq.(1), it can be seen that $S \propto A_{21}/(A+Q)$. For very small quenching rates, the expression represents the branching ratio A_{21}/A of the different fluorescence channels considering an excited level. The motivation to extend our TALIF measurements to the excitation of the $5p^5(^2P^\circ_{1/2})6p\ ^2[3/2]_2$ level at 89162.4 cm^{-1} was the high value of the corresponding branching ratio at the 834.7 nm fluorescence transition of 0.73.[13] (Fig. 2, right panel). Obviously, this is not the only condition to identify an effective TALIF scheme, since the two-photon absorption cross section $\hat{\sigma}^{(2)}$ has also strong influence on the observed fluorescence amplitude. To our knowledge, the two-photon absorption cross section is not documented for this transition. Furthermore, the $5p^5(^2P^\circ_{3/2})7p\ ^2[5/2]_2$ level at 88351.7 cm^{-1} was studied, with the fluorescence detected at 469.7 nm. This level belongs to a multiplet involving the $5p^5(^2P^\circ_{3/2})7p\ ^2[3/2]_2$ state at 88686.5 cm^{-1}, see left panel of Fig.(2) [a]. The corresponding branching ratio is 0.05.[13]

In literature, radiative lifetimes and collisional deactivation rates have been extensively studied for $6p$, $6p'$ and $7p$ systems via two-photon excitation[14,15]. Some lack of data exists for higher multiplets.[b] Note that, besides atom physical interests, the $9p$ system is worth to be investigated as it can serve as a calibration scheme for the 2×211.0 nm transition scheme in atomic nitrogen, if the Xe I two-photon absorption cross section can be determined with sufficient accuracy.[c]

III. Experimental

The experimental setup, in principle, has been described in previous publications[2–4] and is therefore reported briefly. A major change consists in the usage of a Nd:YAG pump laser of shorter pulse time instead of a former excimer laser.

The output of the Nd:YAG (Quantel Brilliant B) pumped Dye Laser (Scanmate 2E) is frequency doubled and focussed by a lens system in a xenon filled cold gas cell. The distance between the focal point and the lens system is ∼150 cm. The pulse duration is ∼ 4.9 ns at a repetition rate of 10 Hz. The wavelength can be adjusted in 0.0005 nm steps for frequency-doubled photons. Laser-induced fluorescence is detected under an angle of 90^o using a gated photomultiplier (Hamamatsu R636-10). The fluorescence signal is collected by an achromatic lens system of f=30 cm at a distance of ∼ 100 cm, representing geometrical conditions for possible ion thruster plasma diagnostics. All fluorescence transitions are detected using interference filters with transmissions of 62% , 52% and 26% at 462.4 nm, 469.7 nm and 834.7 nm respectively.

Data acquisition is managed using a Boxcar Integrator (Stanford Research Systems SR250) and a computer interface (Stanford Research Systems SR245). The laser energy is measured by detecting pulses split from the original beam with an energy monitor (Polytec RjP735). Fluorescence signals are recorded by a 1GHz oscilloscope (Gagescope82G).

IV. Discussion

The three TALIF schemes described in Fig. 2 have been experimentally realized at moderate xenon pressure of $p = 8.5 \cdot 10^{-3}$ mbar in the cold gas cell. Measurements have been performed at moderate pressures in order to reach a regime in which quenching effects do not dominate. The time-resolved fluorescence signal of the $6p'\ ^2[3/2]_2$ state is shown in Fig. 3. In Fig. 4, Stern-Volmer plots of two excited states are given. The extracted lifetime of the $7p\ ^2[3/2]_2$-level is 121 ± 12 ns consistent with the value given by Horiguchi et al[13]. Lifetime of the $7p\ ^2[5/2]_2$-state is 194 ± 23 ns and thus significantly higher than the corresponding value published by Horiguchi et al; but near measurements by Allen et al[18]. However, lifetime measurements differ considerably by several authors, see e.g. Whitehead et al[15] and references herein. Quenching is still a process not to be neglected at $8.5 \cdot 10^{-3}$ mbar, but quenching rates are at least small taking values near or within the error margins of radiative transition rates ($Q_p = 0.32 \cdot 10^6$ s^{-1} for $7p\ ^2[3/2]_2$-level and $Q_p = 0.82 \cdot 10^6$

[a] As an abbreviation, the coupling of the core electrons will be dropped in the the following. To achieve the common notation, an index will be provided when the coupling of the core electrons leads to a $(^2P^\circ_{1/2})$-state to prevent confusion with notation of $(^2P^\circ_{3/2})$ cores. E.g., $5p^5(^2P^\circ_{1/2})6p\ ^2[3/2]_2$ will be shortly written $6p'\ ^2[3/2]_2$.

[b] (nf) levels have been partly investigated in Das and Karmakar[16]. Jiménez et al[17] published lifetimes of some $8p$ levels. In both cases, excitation techniques different from two-photon absorption have been used.

[c] This can be seen as an equivalent to the usage of a two-photon transition to the $5p'$ multiplet in neutral krypton to calibrate atomic nitrogen particle densities excited in a 2×206.6 nm TALIF scheme proposed by Niemi et al[8]

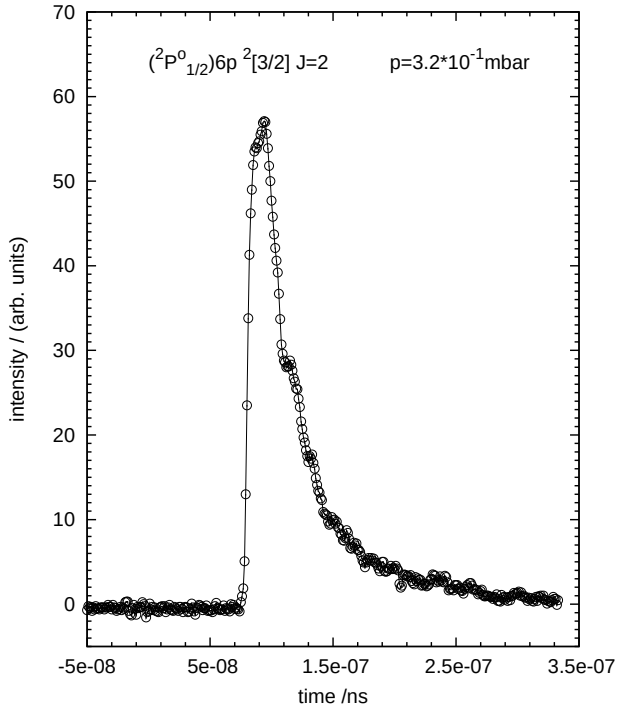

Figure 3. Sample data of the time-dependent fluorescence signal of the $6p'\ ^2[3/2]_2$ level, with fluorescence radiation detected at 834.7 nm.

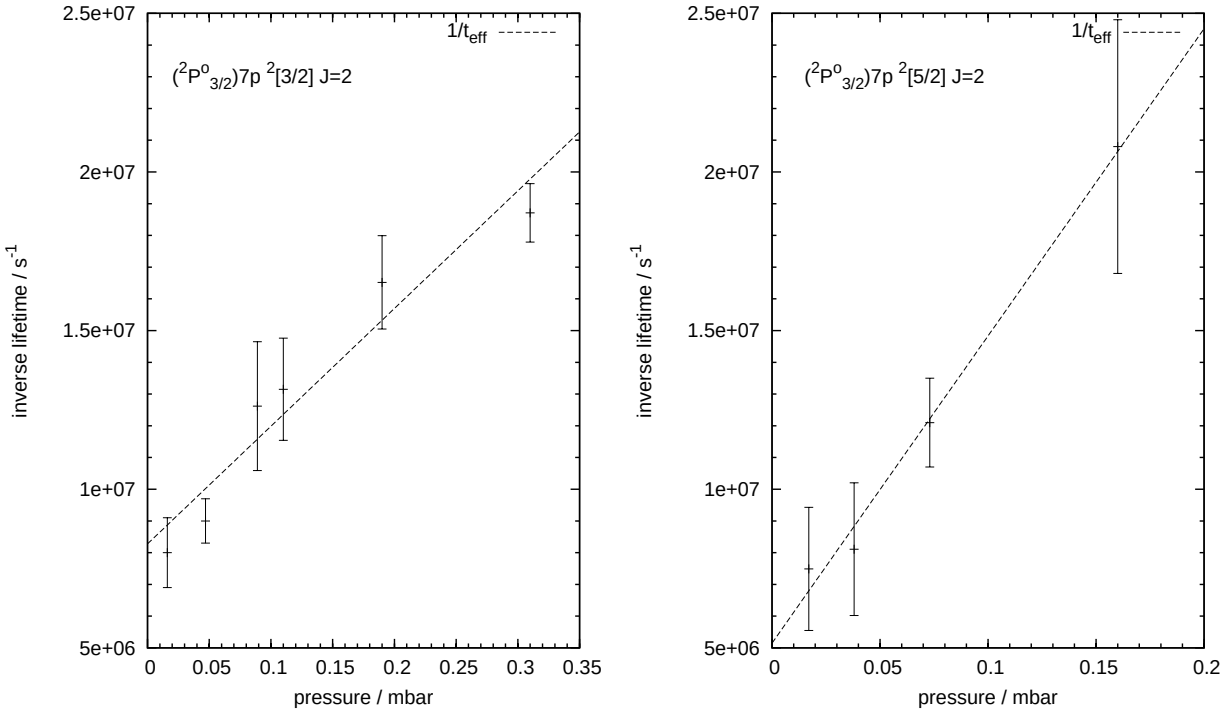

Figure 4. Stern-Volmer-Plots of the excited levels $5p^5(^2P^\circ_{3/2})7p\ ^2[3/2]_2$ (*left*) and $5p^5(^2P^\circ_{3/2})7p\ ^2[5/2]_2$ (*right*).

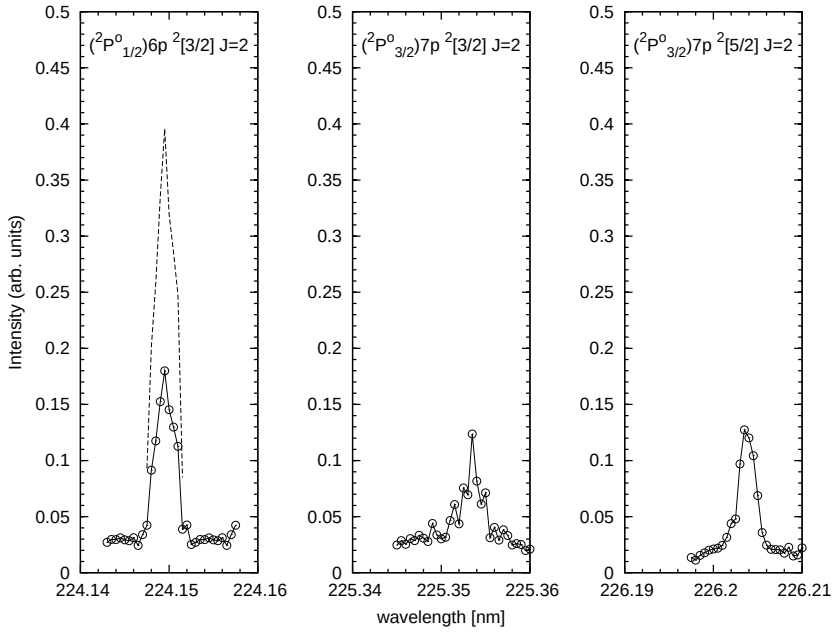

Figure 5. Spectral profiles of the three excited levels, at Xe I pressure $p = 8.5 \cdot 10^{-3}$ mbar each.

s^{-1} for $7p\ ^2[5/2]_2$-level).

In Fig. 5, spectral line-shapes of the fluorescence signals are shown for three excitation schemes. In the present experimental configuration, the line shape is dominated by the broadening of the laser system. Instrumental sensitivities and geometrical factors have been kept constant during the measurements, i.e. the calibration constant varies only in the transmission of the interference filters and the quantum efficiency of the photomultiplier with respect to the fluorescence wavelength. Intensities have been normalized for filter transmission (solid lines). The quantum efficiency of the photomultiplier does not vary significantly for fluorescence detected at 462.4 nm and 469.7 nm ($\eta_\Phi = 0.2$), while being considerably reduced at 834.7 nm ($\eta_\Phi = 0.08$). The dashed line in left panel indicates the signal corrected for different quantum efficiencies. Fluorescence signals at comparable intensities have been measured for all excitation schemes. The fact that fluorescence in the TALIF scheme including the $7p\ ^2[5/2]_2$ appears comparatively strong may be surprising due to the low branching ratio. This is, however, possibly due to a higher two-photon absorption coefficient or different saturation levels, since different two-photon excitation transitions can not be assumed to have the same saturation behavior. Nonetheless, significance of this first measurements is limited, since the quadratic regime (i.e. $S \propto E^2$, cf. equation (1)) was not reached in both alternative excitation schemes. Thus, calculation of relative absorption coefficients can not yield reliable results although all measurements have been taken in the same range of the laser energy. Further investigations are needed, but the experimental set-up has to be changed to allow for lower laser energies at moderate pressures to circumvent saturation effects mentioned above.

V. Some Remarks on Three-Photon Spectroscopy

Unlike the case of Xe I, TALIF can not be used for Xe II spectroscopy since excitation of energy levels with the same parity as the ground state require two photons with $\lambda \lesssim 180$ nm each. Within the wavelength range of available laser systems (including frequency doubling), the energy gap can be overcome by simultaneous absorption of three photons. Selection rules for three photon processes demand for a transition between states of opposite parity. The transition rate between the two levels f and g is

$$W^{(3)}_{f \leftarrow g} = \hat{\sigma}^{(3)} I^3, \tag{3}$$

wherein I is the photon density flux in $cm^{-2}s^{-1}$ and $\hat{\sigma}^{(3)}$ the three-photon absorption cross section in cm^6s^2.

Three-photon spectroscopy on Xe I has been studied experimentally in various publications[5–7], using excitation of the $6s\ ^2[3/2]_1^\circ$ level observing the fluorescence transition back to the ground state at 147 nm. Salamero et al[6] found in their experiments $\hat{\sigma}^{(3)}$ to be of the order 10^{-83} $\mathrm{cm^6 s^2}$. With respect to the two-photon excitation of the $7p\ ^2[3/2]_2$ state, Goehlich et al[9] found $\hat{\sigma}^{(2)}$ to be of the order 10^{-46} $\mathrm{cm^4 s^1}$. Estimating the ratio of transition rates from (3) for a laser of an intensity of 1 $\mathrm{GW/cm^2}$ yields $W^{(3)}/W^{(2)} \sim 10^{-10}$.

Regarding this ratio typical also for Xe II, all further discussion seems to be rather academic. Nevertheless, we would like to point out one potentially interesting aspect. The crucial quantity to know in order to develop a possibly efficient LIF scheme is the (three-photon-) absorption cross section $\hat{\sigma}^{(3)}$. Even for Xe I (as a test case), it seems to be appropriate to find an alternative LIF scheme from the one described previously, as this scheme includes fluorescence observed for a transition back to the ground state (which is not possible in TALIF schemes). Naturally, this is a good choice as the Einstein coefficients $A_{ik} \propto \omega_{ik}^3$, although this dependency is influenced by the transition matrix elements, of course. In resonant processes like this, resonance trapping occurs[5,6], an effect related to the re-absorption of fluorescence photons in the medium itself. This effect is minimized if the detection window is close enough at the focal point (in the order of $\sim 50\mu$m) of the laser beam, which obviously is not practicable for the purposes here. Resonance trapping effects do not occur if excitation transition is allowed for three-photon transitions, but forbidden for one-photon transitions (as e.g. $\Delta J = 3$). For quantitative discussion, the knowledge of $\hat{\sigma}^{(3)}$ is needed.

In quantum mechanics, the absorption cross section is calculated in lowest order perturbation theory by

$$\hat{\sigma}^{(3)} = G^{(3)} g(\omega) 2\pi (2\pi\alpha)^3 \omega^3 \left| \sum_{m_1,m_2} \frac{\langle f|\boldsymbol{\varepsilon}\mathbf{r}|m_1\rangle\langle m_1|\boldsymbol{\varepsilon}\mathbf{r}|m_2\rangle\langle m_2|\boldsymbol{\varepsilon}\mathbf{r}|g\rangle}{(\omega_{m_1} - \omega_g - 2\omega)(\omega_{m_2} - \omega_g - \omega)} \right|^2 . \tag{4}$$

Herein $|m_i\rangle$ represent the complete set of atomic eigenstates, $|f\rangle$ and $|g\rangle$ the final and initial states respectively, ω_i the corresponding eigenfrequencies, ω and $\boldsymbol{\varepsilon}$ the frequency and the polarization of the laser beam, $g(\omega)$ the line profile (including all broadening mechanisms), $G^{(3)}$ the statistical factor and α the fine structure constant. The computation of eq. (4) requires extensive numerical effort since wave functions have to be known with sufficient accuracy even of the continuum states. Wave functions can numerically be found in the Hartree-Fock approximation[19]. Two-photon cross sections have been determined for atomic oxygen using multiconfiguration-interaction codes, e.g. by Saxon and Eichler[20]. However, to our knowledge, there exist no calculations for Xe I and Xe II regarding three-photon transitions. For order-of-magnitude estimations, absorption cross sections can be calculated in the Coulomb-Approximation[21]. An overview is given in the appendix. The procedure can potentially yield useable results within the limitations of the method. However, although our calculations seem to show fairly good agreement with the value given by Salamero[6], the results are not completely consistent since the behavior under variation of numerical parameters is not clear. Naturally, evaluations are extremely difficult to judge due to the lack of existing data. Future reflections may show whether at least trends for different cross sections can be extracted.

VI. Conclusion

TALIF diagnostics on Xe I have been extended to alternative excitation schemes. In first measurements, two excitation schemes besides the "conventional" excitation of $7p\ ^2[3/2]_2$-level (2×225.5 nm) have been applied in a xenon-filled cold gas cell. Lifetime measurements are consistent with values published in literature. Preliminary results with respect to fluorescence intensities show that alternative schemes can be used for TALIF investigations on Xe I equally. To quantify this finding, future work must concentrate on a possible determination of atom specific data such as two-photon absorption coefficients in the non-saturated regime. The study of selected $6p, 8p, 9p, 4f, 5f$-levels is potentially interesting to optimize TALIF diagnostics on Xe I. In addition, some basics of three-photon spectroscopy, with regard of a desirable detection of Xe II, have been discussed. A scheme to estimate related absorption cross sections within lowest-order-perturbation theory and the Coulomb Approximation was given.

Appendix

In the following, an approach to estimate multi-photon absorption cross sections is compiled. The procedure is based on the average-frequency method formulated by Bebb and Gold[22], and, herein, using atomic wave functions in the Coulomb Approximation (CA)[21].

The principles of lowest order perturbation theory have been described in detail elsewhere[22–24]. Therefore, we confine to repeat only the basic steps as far as needed for the purposes in the context of this paper. Assuming one atom in a single laser beam, the probability of simultaneous absorption of N photons in a multi-photon transition between two atomic states $|f\rangle$ and $|g\rangle$ is given by

$$W_{f\leftarrow g}^{(N)} = \hat{\sigma}^{(N)} I^N, \tag{5}$$

wherein $\hat{\sigma}^{(N)}$ denotes the Nth-order transition cross section and I the photon density flux of the laser beam. It is convenient to represent the cross section in terms of a quantity $\sigma_0^{(N)}$ independent of the line-shape and the statistical properties of the laser beam

$$\hat{\sigma}^{(N)} = \sigma_0^{(N)} g(\omega) G^{(N)} \tag{6}$$

with the statistical factor $G^{(N)}$ describing the chaotic properties of the laser beam and the line shape function $g(\omega)$ that includes both the line-shape of the laser beam and all relevant broadening mechanisms[24]. The fundamental quantity $\sigma_0^{(N)}$ is

$$\sigma_0^{(N)} = 2\pi(2\pi\alpha)^N \omega^N |K_{fg}^{(N)}(\omega)|^2 \tag{7}$$

and

$$K_{fg}^{(N)}(\omega) = \sum_{m_{N-1}\cdots m_1} \frac{\langle f|\boldsymbol{\varepsilon}\mathbf{r}|m_{N-1}\rangle\langle m_{N-1}|\boldsymbol{\varepsilon}\mathbf{r}|m_{N-2}\rangle\cdots\langle m_1|\boldsymbol{\varepsilon}\mathbf{r}|g\rangle}{(\omega_{m_{N-1}} - \omega_g - (N-1)\omega)\,(\omega_{m_{N-2}} - \omega_g - (N-2)\omega)\cdots(\omega_{m_1} - \omega_g - \omega)}, \tag{8}$$

wherein the $|m_i\rangle$ represent the complete set of atomic eigenstates, the ω_i the corresponding eigenfrequencies, $\boldsymbol{\varepsilon}$ the polarization vector and ω the frequency of the laser beam, respectively.

In literature, various methods to (approximately) calculate equation (8) have been presented. In the method of Bebb and Gold[22], the infinite summations over all atomic eigenstates are circumvented by introducing so-called average frequencies. The principle of the method shall first be described for the case of a two-photon process, here we have

$$K_{fg}^{(2)}(\omega) = \sum_m \frac{\langle f|\boldsymbol{\varepsilon}\mathbf{r}|m\rangle\langle m|\boldsymbol{\varepsilon}\mathbf{r}|g\rangle}{(\omega_m - \omega_g - \omega)}. \tag{9}$$

An average frequency $\overline{\omega}_m$ can be introduced so that $K_{fg}^{(2)}(\omega)$ can be written in the form

$$K_{fg}^{(2)}(\omega) = \frac{\sum_m \langle f|\boldsymbol{\varepsilon}\mathbf{r}|m\rangle\langle m|\boldsymbol{\varepsilon}\mathbf{r}|g\rangle}{(\overline{\omega}_m - \omega_g - \omega)} = \frac{\langle f|(\boldsymbol{\varepsilon}\mathbf{r})^2|g\rangle}{(\overline{\omega}_1 - \omega)}, \tag{10}$$

where the abbrevation $\overline{\omega}_1 = \overline{\omega}_m - \omega_g$ was used. The last equality is due to the completeness relation $\sum_m |m\rangle\langle m| = 1$ as the summation extends to the complete set of atomic states. Note that the average frequency was defined so that the expression above is exact (with unknown value of $\overline{\omega}_1$, however.) Considering a Nth-order processes, an average frequency can be defined for each summation. Thus it is straightforward to write

$$K_{fg}^{(N)}(\omega) = \frac{\langle f|(\boldsymbol{\varepsilon}\mathbf{r})^N|g\rangle}{\prod_{\nu=1}^{N-1}(\overline{\omega}_\nu - \nu\omega)}, \tag{11}$$

where the average frequency of the νth summation is denoted by $\overline{\omega}_\nu$. An overall average frequency $\overline{\omega}$ can be defined via

$$\prod_{\nu=1}^{N-1}(\overline{\omega}_\nu - \nu\omega) \equiv \prod_{\nu=1}^{N-1}(\overline{\omega} - \nu\omega). \tag{12}$$

Thus the calculation of cross sections has been simplified considerably, as instead of computing the primal infinite summations over matrix elements involving all atomic states, the problem is restricted to the calculation of a single matrix element $\langle f|(\boldsymbol{\varepsilon}\mathbf{r})^N|g\rangle$ wherein "only" the atomic wave functions of the initial and the final states have to be determined. Clearly, the average frequency remains unknown and can, naturally, only be determined exactly by computing the infinite summations in equation (8). In their theoretical work regarding hydrogenic atoms and rare gases, Bebb and Gold[22] found the average frequency can be approximated as the eigenfrequency of the first excited state. It should be kept in mind that this, in general, represents a rather crude estimation, but may yield satisfactory results within the limitations of the method.

However, in the case of many-electron atoms, an accurate calculation of the required wave functions remains an extensive task. To calculate transition matrix elements for one-photon processes, the CA has been used[21,25]. In CA, the excited electron is postulated to move in a central potential that can be approximated to its asymptotic form $\propto r^{-1}$ at moderate and large radial distances, while the transition integral is expected to yield dominant contributions only in this area. Writing the wave function separated in a radial and an angular dependent part,

$$\Psi_{n,l,m} = \mathcal{R}_{nl}(r)Y_{lm}(\theta,\phi). \tag{13}$$

and representing n, l, m the principal, azimuthal and magnetic quantum numbers respectively, the radial part in CA is of the form

$$R(r) = \mathcal{N}(\nu,l)rW_{n,l+1/2}(2Cr/\nu) \tag{14}$$

wherein $R(r) = r\mathcal{R}(r)$ and atomic units have been used; C is the excess charge on the nucleus when one electron is removed, $\nu = C/\sqrt{\epsilon}$ the effective quantum number and ϵ the one-electron energy. $\mathcal{N}(\nu,l)$ is a normalization factor

$$\mathcal{N}(\nu,l) = \frac{C^{1/2}}{[\nu^2\Gamma(\nu+l+1)\Gamma(\nu-l)]^{1/2}}. \tag{15}$$

Note that ν is not necessarily an integer[d] (as it is for hydrogenic problems). $W_{\nu,l+1/2}(Cr/\nu)$ represents the confluent hypergeometric function defined as the solution of the radial Schrödinger equation,

$$\frac{d^2W_{\nu,l+1/2}}{dr^2} + \left[\frac{2C}{r} - \frac{C^2}{\nu^2} - \frac{l(l+1)}{r^2}\right]W_{\nu,l+1/2} = 0. \tag{16}$$

The asymptotic expansion is

$$W_{\nu,l+1/2}(Cr/\nu) = \left(\frac{2Cr}{\nu}\right)^{\nu} e^{-\frac{Cr}{\nu}}\left[1 + \sum_{t=1}^{\infty}\frac{a_t(\nu,l)}{(Cr/\nu)^t}\right] \tag{17}$$

with the coefficients a_t being recursively given through

$$a_t = (\nu/2t)[l(l+1) - (\nu-t)(\nu-t+1)]a_{t-1} \tag{18}$$

and $a_1 = 1$.

It must be emphasized that this approach may only be used to give order-of-magnitude estimations of the quantities related to multi-photon cross sections. However, the procedure is potentially interesting to estimate the cross sections of N-photon processes with $N > 2$.

Acknowledgments

C. Eichhorn wishes to thank the Evangelisches Studienwerk Villigst e.V. for financial and idealistic support through a Ph.D. scholarship. A. Nawaz and A. Knapp are gratefully acknowledged for many helpful comments and essential support with respect to the transportation of the laser system. Research was supported by the Deutsches Zentrum für Luft- und Raumfahrt (DLR).

[d]For non-integer ν, the formula for $\mathcal{N}(\nu,l)$ should be corrected. See Armstrong and Purdum[25] for a short discussion.

References

[1]Löhle, S. and Auweter-Kurtz, M., "Atomic Oxygen Number Density Measurements in Inductively Heated Air Plasma Flows," *Proceedings of the 39th AIAA Plasmadynamics and Lasers Conference*, San Francisco, CA, 5-8 June, AIAA 2006-3759, 2006.

[2]Löhle, S. and Auweter-Kurtz, M., "LIF-Measurements of Atomic Oxygen in Inductively Heated Plasma Flows using two calibration methods," *Journal of Thermophysics and Heat Transfer*, Vol. 21, No. 3, 2007, pp. 623–629.

[3]Löhle, S., "Untersuchungen von Wiedereintrittsplasmen mit Hilfe laserinduzierter Fluoreszenzmessungen", Dissertation, Sierke Verlag, Göttingen, 2006.

[4]Semenova, N., Auweter-Kurtz, M., and Winter, M. W., "Development of Laser-Spectroscopic Techniques on Xenon for RIT-Ion Thruster Plume Investigations," *Proceedings of the 40th Joint Propulsion Conference, Fort Lauderdale, Florida, 11-14 July*, AIAA 2004-3962, 2004.

[5]Faisal, F., Wallenstein, R., and Zacharias, H., "Three-Photon Excitation of Xenon and Carbon Monoxide," *Physical Review Letters*, Vol. 39, No. 18, 1977, pp. 1138–1141.

[6]Salamero, Y., Asselman, H., Birot, A., Brunet, H., Galy, J., and Millet, P., "Multiphoton excitation and frequency tripling in xenon," *Journal of Physics B: Atmic and Molecular Physics*, Vol. 16, 1983, pp. 2971–2979.

[7]Peet, V. and Shchemeljov, S., "Three-photon resonant atomic excitation in spatially incoherent laser beams," *The Physical Review A*, Vol. 68, 2003, pp. 043411/1–043411/6.

[8]Niemi, K., Schulz-von der Gathen, V., and Döbele, H. F., "Absolute calibration of atomic density measurements by laser-induced fluorescence spectroscopy with two-photon excitation," *Journal of Physics D: Applied Physics*, Vol. 34, 2001, pp. 2330–2335.

[9]Goehlich, A., Kawetzki, T., and Döbele, H. F., "On absolute calibration with xenon of laser diagnostic methods based on two-photon absorption," *Journal of Chemical Physics*, Vol. 108, No. 22, 1998, pp. 9362–9370.

[10]Crofton, M. W., "Measurement of Neutral Xenon Density Profile in an Ion Thruster Plume," *Proceedings of the 27th Plasmadynamics and Lasers Conference, New Orleans, LA, 17-20 June*, AIAA 1996-2290, 1996.

[11]Bamford, D. J., Jusinski, L. E., and Bischel, W. K., "Absolute two-photon absorption and three-photon ionization cross sections for atomic oxygen," *Physical Review A*, Vol. 34, No. 1, 1986, pp. 185–198.

[12]Bonin, K. D. and McIlrath, T. J., "Two-photon electric-dipole selection rules," *Journal of the Optical Society of America*, Vol. 1, No. 1, 1984, pp. 52–55.

[13]Horiguchi, H., Chang, R. S. F., and Setser, D. W., "Radiative lifetimes and two-body collisional deactivation rate constants in Ar for Xe($5p^5 6p$),Xe($5p^5 6p'$), and Xe($5p^5 7p$) states," *Journal of Chemical Physics*, Vol. 75, No. 3, 1981, pp. 1207–1218.

[14]Bruce, M. R., Layne, W. B., Whitehead, C. A., and Keto, J. W., "Radiative lifetimes and collisional deactivation of two-photon excited xenon in argon and xenon," *Journal of Chemical Physics*, Vol. 92, No. 5, 1990, pp. 2917–2926.

[15]Whitehead, C. A., Pournasr, H., Bruce, M. R., Cai, H., Kohel, J., Layne, W. B., and Keto, J. W., "Deactivation of two-photon excited Xe($5p^5 6p, 6p', 7p$) and Kr($4p^5 5p$) in xenon and krypton," *Journal of Chemical Physics*, Vol. 102, No. 5, 1995, pp. 1965–1980.

[16]Das, M. B., and Karmakar, S., "Radiative lifetimes of some excited states of neutral xenon," *The European Physical Journal D*, Vol. 32, 2005, pp. 285–288.

[17]Jiménez, E., Campos, J., and Sanchéz del Río, C., "Radiative lifetimes of some levels of XeI and XeII," *Journal of the Optical Society of America*, Vol. 64, No. 7, 1974, pp. 1009–1010.

[18]Allen, L., Jones, D. G. C., and Schofield, D. G., "Radiative Lifetimes and Collisional Quenching Cross Sections for XeI and XeII," *Journal of Chemical Physics*, Vol. 59, No. 7, 1969, pp. 842–847.

[19]Froese Fischer, C., "A general multi-configuration Hartree-Fock program," *Computer Physics Communications*, Vol. 14, 1978, pp. 145–153.

[20]Saxon, R. P. and Eichler, J., "Calculation of two-photon cross sections," *Physical Review A*, Vol. 34, No. 1, 1986, pp. 199–210.

[21]Bates, D. and Damgaard, A., "The Calculation of the Absolute Strengths of Spectral Lines," *Philosophical Transactions of the Royal Society of London. Series A, Mathematical and Physical Sciences*, Vol. 242, No. 842, 1949, pp. 101–122.

[22]Bebb, H. and Gold, A., "Multiphoton Ionization of Hydrogen and Rare-Gas Atoms," *Physical Review*, Vol. 143, No. 1, 1966, pp. 1–24.

[23]Lampropoulos, P., "Topics on Multiphoton Processes in atoms," *Advances in Atom and Molecular Physics*, Vol. 12, 1976, pp. 87–164.

[24]Bräunlich, P., "Multiphoton Spectroscopy," *Progress in Atomic Spectroscopy Part B*, edited by W. Hanle and K. Kleinpoppen, Plenum Press, New York, 1978, pp. 777–827.

[25]Armstrong, B. H. and Purdum, K. L., "Extended Use of the Coulomb Approximation: Mean Powers of r, a Sum Rule, and Improved Transition Integrals," *Physical Review*, Vol. 150, No. 1, 1966, pp. 51–59.